Desalination and Water Treatment
www.deswater.com
doi: 10.1080/19443994.2015.1043490

57 (2016) 10152–10158
May

Taylor & Francis
Taylor & Francis Group

Electrochemical ozone production in inert supporting electrolytes on a boron-doped diamond electrode with a solid polymer electrolyte electrolyzer

Jusol Choi[a], Choonsoo Kim[a], Jiye Kim[a], Seonghwan Kim[a], Yongsug Tak[b], Changha Lee[c,*], Jeyong Yoon[a,*]

[a]*School of Chemical and Biological Engineering, College of Engineering, Institute of Chemical Process, Asian Institute for Energy, Environment & Sustainability (AIEES), Seoul National University (SNU), Gwanak-gu, Daehak-dong, Seoul 151-742, Korea, Tel. +82 2 880 8927; Fax: +82 2 876 8911; email: jeyong@snu.ac.kr (J. Yoon)*
[b]*Department of Chemical Engineering, Inha University, Inchon 402-751, Korea*
[c]*School of Urban and Environmental Engineering, Ulsan National Institute of Science and Technology (UNIST), 100 Banyeon-ri, Eonyang-eup, Ulju-gun, Ulsan 689-798, Korea, Tel. +82 52 217 2812; Fax: +82 52 217 2809; email: clee@unist.ac.kr (C. Lee)*

Received 15 January 2015; Accepted 15 April 2015

ABSTRACT

This study investigated how inert supporting electrolytes (SEs), which increase the electrical conductivity, affect electrochemical ozone production (EOP) on a boron-doped diamond (BDD) electrode. Regardless of the SE species, the EOP was suppressed about 60% in a SE concentration of 1 mM for which the conductivity is similar to that of tap water compared to deionized water. The production of H_2O_2, which is known to be generated by the combination of ·OH, was also suppressed. On the other hand, the formation of ·OH was not significantly affected by the presence of SEs, an intermediate for ozone production. Consequently, suppression of EOP by SE can be explained by physical interference from the diffusion or combination of ·OH by the SE anions concentrated near the electrode surface. This study contributes by providing a better mechanistic understanding of the effect of SEs on EOP in a solid polymer electrolyte/BDD system.

Keywords: Electrochemical ozone production (EOP); Boron-doped diamond (BDD); Solid polymer electrolyte (SPE) electrolyzer; Supporting electrolyte

1. Introduction

Ozone is an environmentally friendly and powerful oxidant because it leaves no harmful by-products after a reaction and has a high redox potential [1,2]. Because of this, it is widely used in a variety of applications, such as disinfection, cleaning, bleaching, wastewater treatment, and water treatment [3,4]. The most common technology for ozone production, the corona discharge process, has several disadvantages such as producing ozone at low concentrations (~2 wt.%) and maintaining a cooling system, drying system, and ozone diffuser [1,5–7]. On the other hand, electrochemical ozone production (EOP) technology has attracted much attention [8] as an alternative to the conventional corona discharge technology. It is an effective and low-cost technology that directly

*Corresponding authors.

Presented at GMVP Desalination Academic Workshop, Seoul, Korea, December 9, 2014

produces a high concentration of ozone in water [3,9]. Electrodes composed of PbO_2 [9–12], SnO_2 [6,13,14], and boron-doped diamond (BDD) with high oxygen overpotential [1,15–17] are popular anode materials for ozone production. Inert supporting electrolytes (SEs) in EOP is essential to provide the electrical conductivity of water electrolysis.

In the case of PbO_2 electrodes, it was reported that highly electronegative anions of SEs improved the current efficiency of EOP [18]. For example, hexafluorophosphate, a highly electronegative anion, enhanced the current efficiency of EOP by more than three times compared to fluoride anions. This observation suggests that less adsorption of more electronegative anions on the electrode surface enables better adsorption of precursors (e.g. oxygen intermediate ·O) and greater production of ozone.

EOP with a solid polymer electrolyte (SPE) electrolyzer combined with a BDD electrode has been investigated by previous studies [1,15,16]. For instance, Kraft's group reported that ozone production was favored by the low conductivity of electrolyzed water with a simple SPE electrolyzer. Arihara's group reported that high-concentration ozone production was achieved (with a current efficiency of 47%) with a perforated BDD/SPE [15], and it was mostly attributed to the improved edge length of the BDD electrodes [1]. In addition, ozone production for small-scale commercial applications was reported with a small-sized generator in a spiral configuration [16]. Despite the high performance of a SPE/BDD electrode system for ozone production, quantitative information and mechanistic explanations as to how the presence of SE affects EOP have not been fully elucidated.

This study investigated how inert SEs affect EOP on a BDD electrode. A SPE electrolyzer was used to permit water oxidation in the absence of SE, i.e. deionized water (DW). EOP, ·OH, and H_2O_2 were measured with the indigo, RNO, and DMP methods, respectively. Based on the suggested mechanisms of EOP [19], the effects of SEs on EOP are discussed.

2. Mechanisms for EOP

Since the first report on EOP from the electrolysis of water by Schönbein [20] in the early 1800s, the mechanism for EOP has been intensively studied. For example, ·OH formation was investigated on PbO_2 electrodes during the EOP process [21], and adsorbed oxygen species on PbO_2 electrodes were deduced [18,22]. Based on the postulation regarding ozone gas phase reactions with low activation energy [22], a commonly accepted mechanism for EOP was suggested by Babak et al., which is as follows [19]:

$$H_2O \rightarrow (^{\cdot}OH)_{ads} + H^+ + e^- \quad (1)$$

$$(^{\cdot}OH)_{ads} \rightarrow (^{\cdot}O)_{ads} + H^+ + e^- \quad (2)$$

$$(^{\cdot}O)_{ads} + (^{\cdot}O)_{ads} \rightarrow (O_2)_{ads} \quad (3)$$

$$(^{\cdot}O)_{ads} + (O_2)_{ads} \rightarrow (O_3)_{ads} \rightarrow O_3 \quad (4)$$

In the case of the PbO_2 electrode, it is suggested that the ·OH generated through the oxidation of water (Reaction (1)) is adsorbed onto the PbO_2 surface leading to ozone production (Reactions (2)–(4)). On the other hand, ·OH is weakly bound to the surface of the BDD electrode compared to the adsorbed ·OH on the PbO_2 surface. As a result, ozone formation on the BDD surface is not favored due to its inert property [23]. In addition, ·OH on the BDD electrode involves the formation of H_2O_2 through a combination of ·OH. (Reaction (5)) [23,24].

$$^{\cdot}OH + {}^{\cdot}OH \rightarrow H_2O_2 \quad (5)$$

3. Materials and methods

All chemicals were of reagent grade and used without any further purification. DW was used in all experiments (<1 μS cm^{-1}, Milli-Q® Direct 8 system, Millipore, Bedford, MA, USA). N,N-dimethyl-p-nitrosoaniline (RNO), 2,9-dimethyl-1,10-phenanthroline (DMP), copper sulfate pentahydrate, and potassium indigo trisulfonate were purchased from Sigma-Aldrich Co. (St. Louis, MO, USA). Five different SEs, potassium hydrogen phosphate (KH_2PO_4), potassium nitrate (KNO_3), perchloric acid ($HClO_4$), sodium fluoride (NaF), and hexafluorophosphoric acid (HPF_6), were used [18,19].

A SPE electrolyzer shown, in Fig. 1, that permits ozone production even in the absence of SEs was used in order to better identify the influence of the SE concentration on EOP. This electrolyzer was manufactured as previously described [25]. The membrane electrode assembly (MEA) consisted of a commercial BDD mesh electrode (apparent surface area: 9.0 cm^2; wire diameter: 0.1 cm, Condias GmbH, Germany) as the anode, Nafion®117 (DuPont, New York, NY, USA) as the SPE, and a 316 stainless steel mesh (apparent surface area: 5.4 cm^2; wire diameter: 0.03 cm) as the cathode. A titanium current collector was used for the BDD electrode, and an Ag/AgCl (KCl sat'd) reference electrode was used. It was confirmed that the titanium current collector did not take part in the electrochemical reactions.

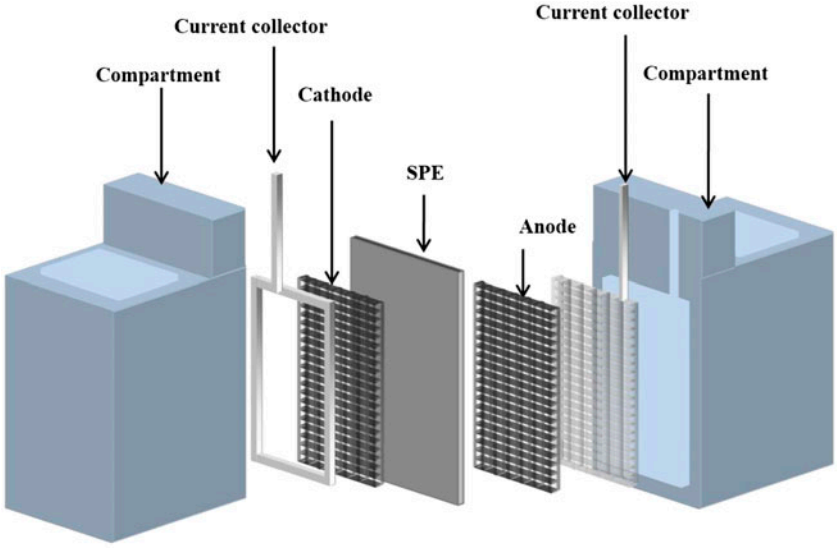

Fig. 1. The configuration of a SPE electrolyzer (working electrode (WE): BDD mesh electrode; counter electrode (CE): stainless steel mesh; reference electrode (RE): Ag/AgCl KCl (sat'd); SPE: Nafion® 117; current collector (CC): titanium).

The effect of individual SEs on EOP with a BDD electrode was conducted for the five different species (KH_2PO_4, KNO_3, $HClO_4$, NaF, and HPF_6) selected as their concentrations were varied from 0.1 to 100 mM. The selected species were relatively inert in this electrochemical system with ·OH. For instance, the fluoride anion is known to be inert during electrolysis, and a relatively slow reaction between $H_2PO_4^-$ and ·OH was reported (rate constant: 2×10^4 L mol^{-1} s^{-1}) [26,27]. Note that a SPE electrolyzer, enabling the electrochemical reaction to occur in conditions of extremely low SE concentrations, was used to investigate the effect of SEs on EOP in a low concentration range. Indeed, the concentrations of the SEs (0.1 mM, DW) in this study were remarkably lower than those in previous studies [18,28]. EOP in the presence of each SE or DW was carried out in the batch mode with stirring under a constant current density of 33 mA cm^{-2} (Potentiostat, Princeton Applied Research, Oak Ridge, TN, USA).

The concentration of ozone was measured with the indigo method and a UV–vis spectrophotometer (Agilent 8453, Agilent Technologies, Santa Clara, CA, USA). The indigo method is based on quantitative decolorization of indigo trisulfonate. This reaction is observed at 600 nm with a detection limit of about 0.01 mg L^{-1} [29]. Then, aqueous ozone was measured at room temperature (20˚C). The effect of a SE on the formation of ·OH was investigated with RNO, an ·OH probe compound [30]. RNO at 0.02 mM was bleached with a constant current density of 33 mA cm^{-2} in the absence or presence of each SE (0.01 mM), and the concentration of RNO was measured over time at 440 nm with a UV–vis spectrophotometer. Then, the observed first-order decay rate constant ($k_{RNO,obs}$) for the reaction of RNO was determined with Eqs. (6) and (7) [31,32] as follows:

$$-\frac{d[RNO]}{dt} = k[^{\cdot}OH]_{ss}[RNO] = k_{RNO\,obs}[RNO] \quad (6)$$

$$-\ln\frac{[RNO]}{[RNO]_0} = k_{RNO,obs}t \quad (7)$$

where [RNO] is the concentration of RNO; $k_{RNO,obs}$ is the $k_{RNO,\cdot OH}$•$[^{\cdot}OH]_{ss}$; $k_{RNO,\cdot OH}$ is the rate constant between ·OH and RNO (1.2×10^{10} M^{-1} s^{-1}, [33]); and $[^{\cdot}OH]_{ss}$ is the steady state concentration of ·OH. This production rate was estimated by the slope of the semi-log plot (Eq. (7)), which was obtained from the assumption of pseudo-first-order kinetics. Note that the magnitude of $k_{RNO,obs}$ represents the extent of the ·OH formation.

To investigate the effect of the SEs on the electrochemical characteristics of water oxidation, cyclic voltammetry was carried out at a scan rate of 160 mV s^{-1} for each individual SE and DW. A stationary cyclic voltammogram of the 20th cycle is presented. In order to examine the effect of the SEs on the formation of H_2O_2 generated through the combination of ·OH, H_2O_2 was measured with the DMP method at 454 nm [34] in 0.01, 1, and 100 mM KNO_3.

4. Results and discussion

Fig. 2 shows the average EOP on the BDD electrode in the presence of the SEs (KH_2PO_4, KNO_3, $HClO_4$, NaF, and $HPF_{6)}$ at varying concentrations (0.01, 1, and 100 mM) and in DW.

The individual plot with standard deviation was drawn by averaging the EOP values for the five SEs. As seen in Fig. 2, three important observations can be addressed. First, the presence of SEs significantly affected the suppression of EOP. EOP decreased about 98, 64, and 22% in 100, 1, and 0.01 mM SE concentrations, respectively, compared to the EOP in DW for 5 min. Second, the type of SE rarely influenced the EOP at each concentration, judging from the small standard deviation. Only the SE concentrations significantly affected the magnitude of the EOP regardless of the type of SE. This observation is also supported by the highest EOP in DW. Third, the EOP for DW is limited because of the high-resistance condition in a conventional electrochemical system. However, with the SPE electrolyzer, the measurement of EOP in DW can be achieved, which enables electrolysis at an extremely low concentration of SE or DW. The electrochemical reaction is possible in the three phase boundary of the SPE electrolyzer: (1) the intersection of the Nafion-H electrolyte (liquid-like phase), (2) the electrodes (solid), and (3) the water (liquid), even without SE [1,25,35].

Fig. 3 shows a representative cyclic voltammogram of the BDD electrode for 100 mM KNO_3 and DW (the inset: 0.01 mM KNO_3 and DW, 160 mV s^{-1}). Although

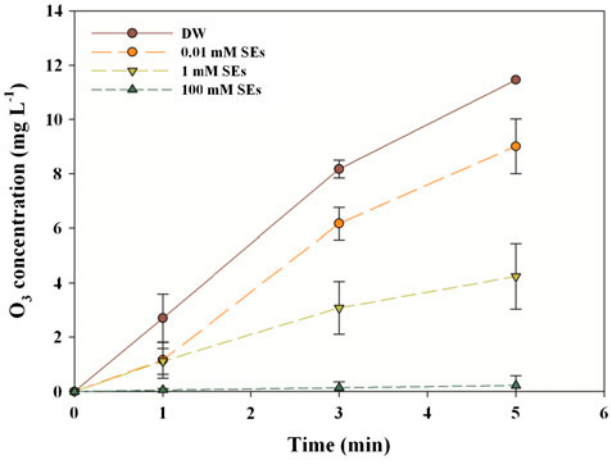

Fig. 2. The average EOP on the BDD electrode in the presence of SEs (KH_2PO_4, KNO_3, $HClO_4$, NaF, and HPF_6) at varying concentrations (0.01, 1, and 100 mM) and in the DW. The individual plot with standard deviation was presented by averaging the EOP values in five SEs (33 mA cm^{-2}).

the EOP was overwhelmingly suppressed at the high concentration of KNO_3 (100 mM) compared to that in DW (Fig. 2), the anodic current density increased substantially at 2.0–3.0 V vs. Ag/AgCl KCl (sat'd). Furthermore, similar cyclic voltammogram trends were observed in the other SEs ($HClO_4$, NaF, HPF_6, and KH_2PO_4) (refer to Fig. S1 in SI). On the other hand, at low concentration of SEs (0.01 mM), the anodic current density was similar to that in DW shown in the inset in Fig. 3. This result suggests that the EOP decrease at a high concentration of SEs did not result from the suppression of electrolysis (Reaction (1)). As mentioned earlier, electrolysis can occur on both the whole electrode surface and the three phase boundary, leading to an increase in the anodic current density in the presence of the SEs.

Table 1 shows the observed first-order decay rate constants ($k_{RNO,obs}$) of the reaction with RNO in aqueous solution containing five the different electrolytes and DW (a SPE electrolyzer, 33 mA cm^{-2}, 0.01 mM, 30 s). As shown in Table 1, the values of $k_{RNO,obs}$ in the presence of the SEs were higher than that in DW regardless of the type of SEs, indicating an increase in the formation of ·OH in the SEs. Overall, in the presence of the SEs, the increase in anodic current density in Fig. 3 and ·OH formation in Table 1 suggest that Reaction (1) cannot be suppressed by the anions of the SEs. In contrast, the EOP was suppressed in the presence of the SEs in Fig. 2. As a result, it can be interpreted that the anions in the SEs do not interfere with the electrolysis (Reaction (1)) even at a low concentration and significantly affect other reactions (Reactions (2)—(4)).

Fig. 4 shows the production of H_2O_2 in 0.01, 1, and 100 mM KNO_3 and DW, which can be generated through the combination of ·OH solution. As can be seen in Fig. 4, the production of H_2O_2 was greatly inhibited as the concentration of KNO_3 increased in accordance with the tendency of EOP (Fig. 2). The H_2O_2 productions decreased about 98, 64, and 22% for the 100, 1, and 0.01 mM SE concentration (KNO_3), respectively, compared to the EOP in DW for 5 min. Although ·OH formation is not suppressed even at a low concentration for the SEs (Table 1), the H_2O_2 formation remarkably decreased. This result indicates that the combination of ·OH on the BDD electrode is also being hindered by the anions in the SEs (Reaction (5)).

Consequently, the results of this study propose that the inert anions near the BDD electrode surface significantly affect EOP. Because the anions are densely packed, the diffusion or combination of ·OH can be hindered at a high concentration of SE. On the other hand, ·OH on the BDD surface at a low

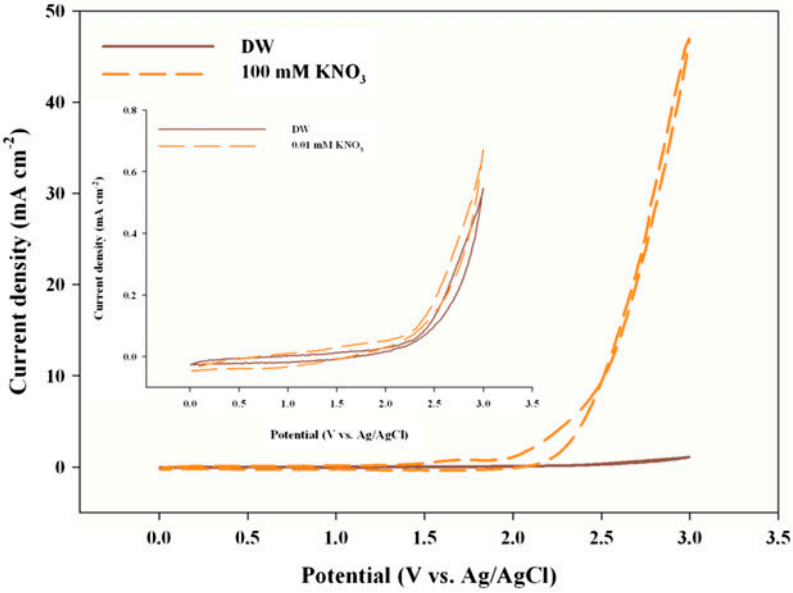

Fig. 3. Cyclic voltammograms on the BDD electrode in 100 mM KNO_3 compared to that in DW (the inset: 0.010 mM KNO_3, 160 mVs^{-1}, the SPE electrolyzer).

Table 1
The observed first-order decay rate constants ($k_{RNO,obs}$) of the reaction with RNO in an aqueous solution containing the SEs (0.01 mM) compared to that in DW (a constant current of 33 mA cm^{-2}, 30 s, SPE electrolyzer)

	$k_{RNO,obs}$[a] ($\times 10^{-2}$ s^{-1})
DW	3.5 ± 0.1
KNO_3	5.7 ± 0.2
KH_2PO_4	6.2 ± 0.6
$HClO_4$	5.3 ± 0.8
NaF	5.2 ± 0.2
HPF_6	5.5 ± 0.2

[a]$k_{RNO,obs}$ = the $k_{RNO,\cdot OH}$ $[\cdot OH]_{ss}$ ($k_{RNO,}$·OH) is the rate constant between ·OH and RNO (1.2×10^{10} M^{-1} s^{-1}), and $[\cdot OH]_{ss}$ is the steady state concentration of ·OH.

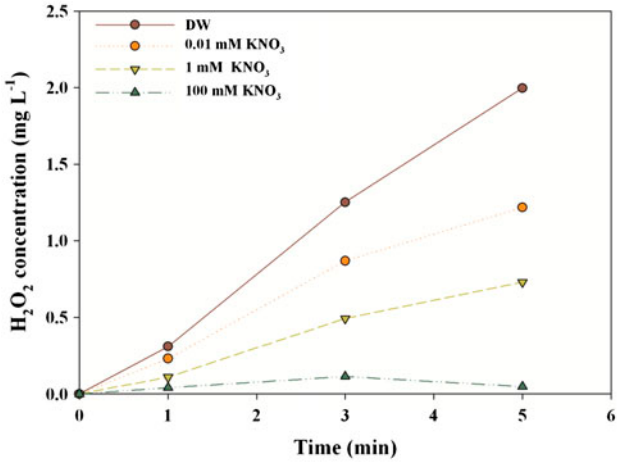

Fig. 4. Electrochemical production of H_2O_2 on the BDD electrode in the presence of KNO_3 (0.01, 1, and 100 mM) compared to that in DW (33 mA cm^{-2}, the SPE electrolyzer).

concentration can feasibly diffuse to the bulk and react with the adjacent ·OH with less hindrance from the SE anions.

5. Conclusion

In this study, the effect of the inert SE in EOP on a BDD electrode was investigated quantitatively. Although ·OH formation was not inhibited even at a low concentration of SEs, the presence of the selected SEs caused a significant suppression of EOP on the BDD regardless of the SE type. This suppression of EOP on the BDD electrode is explained by the interference from the diffusion or combination of ·OH with the SE anions concentrated near the electrode surface. This mechanism is supported by the suppression of H_2O_2 production. Furthermore, EOP in DW was measured with a SPE electrolyzer, which enables electrolysis in an extremely low concentration of SE and DW. Therefore, this study contributes by providing a better understanding on the effect of SEs on EOP in a SPE/BDD system.

Supplementary material

The supplementary material for this paper is available online at http://dx.doi.10.1080/19443994.2015.1043490.

Acknowledgement

This research was supported by a grant from Industrial Facilities & Infrastructure Research Program funded by Ministry of Land, Infrastructure and Transport of Korean government (grant number 13IFIP-B065893-01).

References

[1] K. Arihara, C. Terashima, A. Fujishima, Electrochemical production of high-concentration ozone-water using freestanding perforated diamond electrodes, J. Electrochem. Soc. 154 (2007) E71–E75.
[2] S. Stucki, G. Theis, R. Kötz, H. Devantay, H. Christen, *In situ* production of ozone in water using a membrel electrolyzer, J. Electrochem. Soc. 132 (1985) 367–371.
[3] K. Onda, T. Ohba, H. Kusunoki, S. Takezawa, D. Sunakawa, T. Araki, Improving characteristics of ozone water production with multilayer electrodes and operating conditions in a polymer electrolyte water electrolysis cell, J. Electrochem. Soc. 152 (2005) D177–D183.
[4] S. Stucki, H. Baumann, H. Christen, R. Kötz, Performance of a pressurized electrochemical ozone generator, J. Appl. Electrochem. 17 (1987) 773–778.
[5] L.M.d. Silva, M.H. Santana, J.F. Boodts, Electrochemistry and green chemical processes: Electrochemical ozone production, Quim. Nova 26 (2003) 880–888.
[6] Y. Cui, Y. Wang, B. Wang, H. Zhou, K.-Y. Chan, X.-Y. Li, Electrochemical generation of ozone in a membrane electrode assembly cell with convective flow, J. Electrochem. Soc. 156 (2009) E75–E80.
[7] L.M.d. Silva, W.F. Jardim, Trends and strategies of ozone application in environmental problems, Quim. Nova, 29 (2006) 310–317.
[8] P.A. Christensen, T. Yonar, K. Zakaria, The electrochemical generation of ozone: A review, Ozone Sci. Eng. 35 (2013) 149–167.
[9] L.M. Da Silva, D.V. Franco, L.G. Sousa, I.C. Gonçalves, Characterization of an electrochemical reactor for the ozone production in electrolyte-free water, J. Appl. Electrochem. 40 (2010) 855–864.
[10] L.M. Da Silva, D.V. Franco, J.C. Forti, W.F. Jardim, J.F. Boodts, Characterisation of a laboratory electrochemical ozonation system and its application in advanced oxidation processes, J. Appl. Electrochem. 36 (2006) 523–530.
[11] R. Amadelli, L. Armelao, A. Velichenko, N. Nikolenko, D. Girenko, S. Kovalyov, F. Danilov, Oxygen and ozone evolution at fluoride modified lead dioxide electrodes, Electrochim. Acta 45 (1999) 713–720.
[12] P. Tatapudi, J.M. Fenton, Synthesis of ozone in a proton exchange membrane electrochemical reactor, J. Appl. Electrochem. 140 (1993) 3527–3530.
[13] Y.-H. Wang, S. Cheng, K.-Y. Chan, X.Y. Li, Electrolytic generation of ozone on antimony- and nickel-doped tin oxide electrode, J. Electrochem. Soc. 152 (2005) D197–D200.
[14] S.-A. Cheng, K.-Y. Chan, Electrolytic generation of ozone on an antimony-doped tin dioxide coated electrode, Electrochem. Solid-State Lett. 7 (2004) D4–D6.
[15] A. Kraft, M. Stadelmann, M. Wunsche, M. Blaschke, Electrochemical ozone production using diamond anodes and a solid polymer electrolyte, Electrochem. Commun. 8 (2006) 883–886.
[16] Y. Nishiki, N. Kitaori, K. Nakamuro, Performances of small-sized generator of ozone-dissolved water using boron-doped diamond electrodes, Ozone Sci. Eng. 33 (2011) 114–120.
[17] E. Brillas, C.A.M. Huitle, Synthetic Diamond Films: Preparation, Electrochemistry, Characterization and Applications, Wiley, New York, NY, 2011.
[18] P.C. Foller, C.W. Tobias, The anodic evolution of ozone, J. Electrochem. Soc. 129 (1982) 506–515.
[19] A. Babak, R. Amadelli, A. De Battisti, V. Fateev, Influence of anions on oxygen/ozone evolution on PbO_2/*spe* and PbO_2/Ti electrodes in neutral pH media, Electrochim. Acta 39 (1994) 1597–1602.
[20] M.B. Rubin, The history of ozone: The Schönbein period, 1839–1868, Bull. Hist. Chem 26 (2001) 40–56.
[21] D. Wabner, C. Grambow, Reactive intermediates during oxindation of water lead dioxide and platinum electrodes, J. Electroanal. Chem. 195 (1985) 95–108.
[22] E. Kötz, S. Stucki, Ozone and oxygen evolution on PbO_2 electrodes in acid solution, J. Electroanal. Chem. 228 (1987) 407–415.
[23] P. Michaud, M. Panizza, L. Ouattara, T. Diaco, G. Foti, C. Comninellis, Electrochemical oxidation of water on synthetic boron-doped diamond thin film anodes, J. Appl. Electrochem. 33 (2003) 151–154.
[24] B. Marselli, J. Garcia-Gomez, P.-A. Michaud, M. Rodrigo, C. Comninellis, Electrogeneration of hydroxyl radicals on boron-doped diamond electrodes, J. Electrochem. Soc. 150 (2003) D79–D83.
[25] I. Yamanaka, T. Murayama, Neutral H_2O_2 synthesis by electrolysis of water and O_2, Angew. Chem. Int. Ed. 120 (2008) 1926–1928.
[26] J.J. Wu, S.J. Masten, Oxidation kinetics of phenolic and indolic compounds by ozone: Applications to synthetic and real swine manure slurry, Water Res. 36 (2002) 1513–1526.
[27] S.J. Masten, M.J. Galbraith, S.H. Davies, Oxidation of 1, 3, 5-trichlorobenzene using advanced oxidation processes, Ozone Sci. Eng. 18 (1996) 535–547.
[28] L.M. Da Silva, L.A. De Faria, J.F. Boodts, Electrochemical ozone production: Influence of the supporting electrolyte on kinetics and current efficiency, Electrochim. Acta 48 (2003) 699–709.
[29] H. Bader, J. Hoigné, Determination of ozone in water by the indigo method, Water Res. 15 (1981) 449–456.
[30] C. Comninellis, Electrocatalysis in the electrochemical conversion/combustion of organic pollutants for waste water treatment, Electrochim. Acta 39 (1994) 1857–1862.
[31] M. Cho, H. Chung, W. Choi, J. Yoon, Linear correlation between inactivation of *E. coli* and OH radical concentration in TiO_2 photocatalytic disinfection, Water Res. 38 (2004) 1069–1077.

[32] C. Lee, J. Yoon, Temperature dependence of hydroxyl radical formation in the $h\nu/Fe^{3+}/H_2O_2$ and Fe^{3+}/H_2O_2 systems, Chemosphere 56 (2004) 923–934.
[33] G.V. Buxton, C.L. Greenstock, W.P. Helman, A.B. Ross, Critical review of rate constants for reactions of hydrated electrons, hydrogen atoms and hydroxyl radicals ($^{\cdot}OH/^{\cdot}O^{-}$ in aqueous solution, J. Phys. Chem. Ref. Data 17 (1988) 513–886.
[34] A.N. Baga, G. Johnson, N.B. Nazhat, R.A. Saadalla-Nazhat, A simple spectrophotometric determination of hydrogen peroxide at low concentrations in aqueous solution, Anal. Chim. Acta 204 (1988) 349–353.
[35] Y. Zhang, C. Wang, N. Wan, Z. Liu, Z. Mao, Study on a novel manufacturing process of membrane electrode assemblies for solid polymer electrolyte water electrolysis, Electrochem. Commun. 9 (2007) 667–670.